Atmospheric
Chemistry
and Physics

Modeling the impact of chlorine emissions from coal combustion and prescribed waste incineration on tropospheric ozone formation in China

Yiming Liu[1,2], Qi Fan[1,2], Xiaoyang Chen[1,2], Jun Zhao[1,2], Zhenhao Ling[1,2], Yingying Hong[3], Weibiao Li[1,2], Xunlai Chen[4], Mingjie Wang[4], and Xiaolin Wei[4]

[1]School of Atmospheric Sciences, Sun Yat-sen University, Guangzhou, 510275, China
[2]Guangdong Province Key Laboratory for Climate Change and Natural Disaster Studies, Guangzhou, 510275, China
[3]Guangdong Ecological Meteorology Center, Guangzhou, 510640, China
[4]Shenzhen Key Laboratory of Severe Weather in South China, Shenzhen, 518040, China

Correspondence: Qi Fan (eesfq@mail.sysu.edu.cn) and Jun Zhao (zhaojun23@mail.sysu.edu.cn)
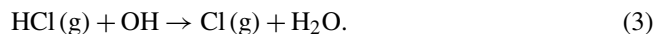
Abstract. Chlorine radicals can enhance atmospheric oxidation, which potentially increases tropospheric ozone concentration. However, few studies have been done to quantify the impact of chlorine emissions on ozone formation in China due to the lack of a chlorine emission inventory used in air quality models with sufficient resolution. In this study, the Anthropogenic Chlorine Emissions Inventory for China (ACEIC) was developed for the first time, including emissions of hydrogen chloride (HCl) and molecular chlorine (Cl_2) from coal combustion and prescribed waste incineration (waste incineration plant). The HCl and Cl_2 emissions from coal combustion in China in 2012 were estimated to be 232.9 and 9.4 Gg, respectively, while HCl emission from prescribed waste incineration was estimated to be 2.9 Gg. Spatially the highest emissions of HCl and Cl_2 were found in the North China Plain, the Yangtze River Delta, and the Sichuan Basin. Air quality model simulations with the Community Multiscale Air Quality (CMAQ) modeling system were performed for November 2011, and the modeling results derived with and without chlorine emissions were compared. The magnitude of the simulated HCl, Cl_2 and $ClNO_2$ agreed reasonably with the observation when anthropogenic chlorine emissions were included in the model. The inclusion of the ACEIC increased the concentration of fine particulate Cl^-, leading to enhanced heterogeneous reactions between Cl^- and N_2O_5, which resulted in the higher production of $ClNO_2$. Photolysis of $ClNO_2$ and Cl_2 in the morning and the reaction of HCl with OH in the afternoon produced chlorine radicals which accelerated tropospheric oxidation. When anthropogenic chlorine emissions were included in the model, the monthly mean concentrations of fine particulate Cl^-, daily maximum 1 h $ClNO_2$, and Cl radicals were estimated to increase by up to about $2.0 \, \mu g \, m^{-3}$, 773 pptv, and 1.5×10^3 molecule cm^{-3} in China, respectively. Meanwhile, the monthly mean daily maximum 8 h O_3 concentration was found to increase by up to 2.0 ppbv (4.1 %), while the monthly mean NO_x concentration decreased by up to 0.5 ppbv (6.1 %). The anthropogenic chlorine emissions potentially increased the 1 h O_3 concentration by up to 7.7 ppbv in China. This study highlights the need for the inclusion of anthropogenic chlorine emission in air quality modeling and demonstrated its importance in tropospheric ozone formation.
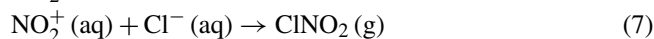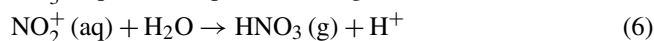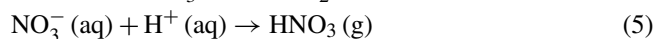
1 Introduction

Chlorine radicals (Cl) are highly reactive, playing a significant role in the oxidative chemistry of the troposphere (Faxon and Allen, 2013; Young et al., 2014). Similar to hydroxyl radicals (OH), chlorine radicals can oxidize volatile organic compounds (VOCs), which potentially enhance ozone formation. In general, chlorine radicals are more reactive towards most of the VOCs than hydroxyl radicals. The reaction rate constants of chlorine radicals with many alkanes, aromatics, alcohols, and ethers range typically between 1 and

2 orders of magnitude greater than the corresponding values for hydroxyl radicals (Aschmann and Atkinson, 1995; Nelson et al., 1990; Wang et al., 2005). Hence, the high reaction rates make the chlorine radicals competitive with the OH radicals though the concentration of chlorine radicals is an order of magnitude or more lower than that of hydroxyl radicals (Wingenter et al., 1999). Chlorine radicals can be produced from photodissociation and oxidation of many of the most common chlorinated organic species, but these reaction rates are generally not fast enough to contribute significantly to the concentrations of chlorine radicals. $ClNO_2$, Cl_2, and HCl are dominant primary chlorine radical sources. Riedel et al. (2012) reported that the relative contributions to Cl radicals from $ClNO_2$, Cl_2, and HCl were approximately 45, 10, and 45 %, respectively, in the Los Angeles regions by using a simple box model with local observation. While photolysis of $ClNO_2$ and Cl_2 occurs in the morning, the reaction of HCl with OH occurs in the afternoon. The reactions are shown as follows:

$$ClNO_2\,(g) + h\nu \rightarrow Cl\,(g) + NO_2\,(g) \tag{1}$$

$$Cl_2\,(g) + h\nu \rightarrow 2Cl\,(g) \tag{2}$$

$$HCl\,(g) + OH \rightarrow Cl\,(g) + H_2O. \tag{3}$$

In the troposphere, nitryl chloride is formed primarily by the heterogeneous reaction between N_2O_5 and Cl^- (Eqs. 4–7) (Bertram and Thornton, 2009; Roberts et al., 2009), while the latter reactant Cl^- is the major product of HCl neutralization (Seinfeld and Pandis, 1998; Pio and Harrison, 1987). Therefore, identification of emission sources and quantification of their contributions to ambient HCl levels are of critical importance for the estimation of the abundance of $ClNO_2$ and/or Cl radicals.

$$N_2O_5\,(g) \leftrightarrow NO_3^-\,(aq) + NO_2^+\,(aq) \tag{4}$$

$$NO_3^-\,(aq) + H^+\,(aq) \rightarrow HNO_3\,(g) \tag{5}$$

$$NO_2^+\,(aq) + H_2O \rightarrow HNO_3\,(g) + H^+ \tag{6}$$

$$NO_2^+\,(aq) + Cl^-\,(aq) \rightarrow ClNO_2\,(g) \tag{7}$$
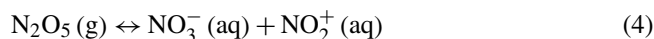
The major sources of tropospheric HCl in the atmosphere include natural sources from sea salt (Keene et al., 1999) and biomass burning (Andreae et al., 1996) and anthropogenic sources from coal combustion and waste incineration (McCulloch et al., 1999). The global annual emission rates of HCl from sea salt and biomass burning were estimated to be 50 Tg Cl yr^{-1} (Graedel and Keene, 1995; Keene et al., 1999) and 6 Tg Cl yr^{-1} (Lobert et al., 1999), respectively. Although the emission rates from natural sources are much higher than their anthropogenic counterparts, they are relatively constant and well estimated. The corresponding anthropogenic emission rates from coal combustion and waste incineration were previously estimated to be 4.6 and 2 Tg Cl yr^{-1}, respectively (McCulloch et al., 1999). Waste incinerations include open waste incineration (the uncontrolled emissions from both residential and dump waste burning) and prescribed waste incineration (the emission from waste incineration plant). The

contribution of open waste incineration to HCl was estimated to be 1 Tg yr^{-1} in China (Wiedinmyer et al., 2014), while that of prescribed waste was unknown, awaiting further investigation.

Molecular chlorine (Cl_2) is another important precursor of Cl radicals. However, only a few studies on its emissions are available in the literature. Chang et al. (2002) compiled an emission inventory of Cl_2 and HOCl for Houston and estimated an emission of about 10^4 kg per day in total in southeast Texas. Deng et al. (2014) collected flue gas samples from six pulverized coal boiler units of four coal-fired power plants in China and found that about 3.6 % of chlorine in coal could release in the form of gaseous Cl_2 during combustion. Measurements of Cl_2 in urban environment are also sparse, although some were made in marine air and at polar sunrise in the past (Finley and Saltzman, 2008; Lawler et al., 2011; Spicer et al., 2002; Impey et al., 1997).

Once the chlorine emission inventory was constructed, the effects of the chlorine radicals on tropospheric ozone formation can be assessed with air quality models by incorporating the emission inventory. For example, the simulation results of the comprehensive air quality model with extensions (CAMx) found that the emissions of HCl and HOCl could increase 1 h averaged O_3 concentration by 70 ppbv in very localized areas during morning hours (Chang and Allen, 2006). Furthermore, Sarwar and Bhave (2007) estimated the effect of chlorine emission on ozone formation in the eastern United States through model simulations. They found that the monthly mean daily maximum 1 h ozone mixing ratios could be enhanced by up to 3 ppbv in the Houston area when the anthropogenic emissions of Cl_2 and HOCl and the chlorine from sea salt aerosols were considered.

However, the role of the oxidation of hydrocarbons by Cl radicals on O_3 formation is still unclear in China, which is mainly due to the lack of an up-to-date anthropogenic chlorine emission inventory. For example, the most widely used emission inventory, the Multi-resolution Emission Inventory for China (MEIC), which was developed by Tsinghua University (http://www.meicmodel.org), does not include HCl and Cl_2 emissions. In addition, though a reactive chlorine emission inventory (RCEI) in 1990 from coal combustion and waste burning was developed by McCulloch et al. (1999), covering each country all around the world with a resolution of $1° \times 1°$, it could not represent the present situation in China due to the fast industrial and economic development in recent years. Li et al. (2016) applied the RCEI in the WRF-Chem (Weather Research and Forecasting coupled with Chemistry) model to simulate the air quality in the Pearl River Delta of China. Results from sensitivity experiments showed that the simulated particulate Cl^- and $ClNO_2$ concentrations were highly sensitive to the chlorine emissions. There is hence a need to develop an up-to-date anthropogenic chlorine emission inventory in China in order to better model $ClNO_2$ production and to quantify its effect on atmospheric chemistry and air quality. Development of an anthropogenic

chlorine emission inventory can also help policymakers to propose better strategies in air quality management.

In this study, the Anthropogenic Chlorine Emission Inventory for China (ACEIC) was developed for the first time to include the emissions of hydrogen chloride and molecular chlorine from coal combustion and prescribed waste incineration in China. This emission inventory was then applied to the Community Multiscale Air Quality (CMAQ) modeling system to evaluate the effects of chlorine emissions on photochemical O_3 formation through sensitivity analysis. Simulations were performed for November 2011 and the results derived with and without the ACEIC were compared. Section 2 describes the development of chlorine emissions in China. Section 3 presents the model simulation to quantify the impact of these anthropogenic chlorine emissions on atmospheric oxidation and ozone formation.

2 Chlorine emission inventory for China

2.1 Emission from coal combustion

2.1.1 Coal consumption database

Coal consumption data are needed for estimating the chlorine emissions. We selected 2012 as the base year of this emission inventory. The database of coal consumptions was constructed based on the data from the China Energy Statistical Yearbook (CESY, National Bureau of Statistics, 2013), which include 31 provinces, municipalities, and autonomous regions. A zero value of coal consumption in Tibet was assumed in the database due to unavailable data in the yearbook. In addition, coal combustion in Hong Kong and Taiwan were taken from International Energy Agency energy statistics (IEA, 2012) and were included in the database. Hence a total of 33 regions were included in this inventory (Table 1). Similar to the classification method used in the MEIC emission inventory, in the ACEIC we classified the coal consumption from the CESY into four economic sectors according to their characteristics: (1) power plant sector, including electricity plants, heat plants, and combined heat and power (CHP) plants; (2) industrial sector, including iron and steel, nonferrous metals, and other categories covering large-scale combustion processes; (3) residential sector, including personal consumption in both urban and rural regions; (4) other sector, including agriculture, forestry, animal husbandry, fishery, water conservancy, construction, transport, storage, post, wholesale, retail trade, hotel, restaurants, and other consumption. Columns 2–5 in Table 1 list the coal consumption among different categories in different provinces (or regions), along with various chlorine content in coal as discussed in the following section. In 2012, a total of 3.6 million tons of coal were consumed, with Shandong (0.3 million tons) being the highest consumer and Hainan the lowest (about 9000 t, Tibet not included).

2.1.2 Chlorine contents in coal

Chlorine is enriched in coal to some extent and is volatilized during the coal combustion process. The chlorine content in coal is essential for emission estimation and it can vary from region to region. It was reported that the chlorine content in coal in China ranged from 50 to 500 $\mu g\,g^{-1}$ with an average value of $\sim 220\,\mu g\,g^{-1}$ (Tang and Chen, 2002), lower than most other countries. Meanwhile, average chlorine contents between 200 and 300 $\mu g\,g^{-1}$ in China were also reported (Lu, 1996; Zhao et al., 1999). Chen (2010) reported a wide range of chlorine content (39–637 $\mu g\,g^{-1}$) with an average chlorine content of 280 $\mu g\,g^{-1}$, falling within the values mentioned above. In this study, we chose chlorine contents reported from Chen (2010) to estimate chlorine emissions in all regions except Shanghai, Tianjin, Hong Kong, and Taiwan. For these regions where chlorine contents are not listed in the literature, we estimated the chlorine emissions using the average chlorine content (280 $\mu g\,g^{-1}$) in China according to Chen (2010).

Some of the coals consumed in China were imported from other countries which might have different chlorine contents. According to the report of the China Energy Statistical Yearbook (CESY, National Bureau of Statistics, 2013), the total amount of coals imported into China was 288 Tg and the total coal consumption in China was 3526 Tg in 2012. Over 91 % of the coals were domestically produced in China. It is hence concluded that the different chlorine content of the imported coals has a minor influence on the estimation of chlorine emission in China. However, it is difficult to evaluate the extent of this influence. Hence, we estimated the chlorine emission from coal combustion in China using the chlorine content of coal from domestic sources and did not take the different chlorine content of the imported coals into account.

2.1.3 Chlorine emission factors

Chlorine emission factors from coal combustion vary with boilers and removal facilities. Table 2 summarizes the chlorine emission factors depending on the combination of boiler types and pollution control technologies in coal combustion (Jiang et al., 2005). This combination can vary significantly from one sector to another.

The net emission factors (EFs) were estimated by the following Eq. (8):

$$EF_{i,j} = c_i \times \sum_k \left(R_{j,k} \times X_{j,k} \times \left(1 - \eta_{d_{j,k}}\right) \times \left(1 - \eta_{s_{j,k}}\right) \right), \quad (8)$$

where i represents the province (municipality, autonomous region), j represents the economic sector, k represents the energy allocation type (type of boiler and control device combination), c represents chlorine contents in coal, R is the chlorine release rate, X is the fraction of energy for a sector (energy allocation ratio), η_d is the removal efficiency of dust-removal facilities, and η_s is the removal efficiency of

Table 1. Coal consumption and emissions of hydrogen chloride and molecular chlorine, listed alphabetically according to regions.

Region	Coal consumption (Gg)				Chlorine content in coal (µg g⁻¹)	HCl emission from coal consumption (Mg)					Cl₂ emission from coal consumption (Mg)					Waste incineration (Gg)	HCl emission from waste incineration (Mg)
	Power	Industry	Residential	Other		Power	Industry	Residential	Other	Total	Power	Industry	Residential	Other	Total		
Anhui	108 519	30 508	530	628	132	479	2213	58	73	2823	19	89	2	3	114	1159	86
Beijing	12 574	3967	2722	3446	90	38	196	204	272	711	2	8	8	11	29	947	70
Chongqing	17 806	32 342	1941	5142	617	369	10 998	999	2788	15 154	15	444	40	113	612	950	70
Fujian	47 660	32 767	790	987	39	62	703	26	34	824	3	28	1	1	33	2501	185
Gansu	38 760	14 486	5157	1891	250	325	1992	1074	415	3805	13	80	43	17	154		
Guangdong	118 779	53 382	636	1071	67	266	1962	35	63	2325	11	79	1	3	94	4947	367
Guangxi	32 622	31 182	368	1188	270	296	4644	83	282	5305	12	187	3	11	214	269	20
Guizhou	54 049	35 384	8772	13 929	165	299	3214	1206	2017	6736	12	130	49	81	272		
Hainan	6914	2392	0	0	67	15	88	0	0	103	1	4	0	0	4	616	46
Hebei	111 357	74 229	13 945	7355	310	1157	12 671	3603	2002	19 433	47	512	145	81	785	1255	93
Heilongjiang	64 369	24 149	4037	12 274	194	418	2577	652	2088	5735	17	104	26	84	232	92	7
Henan	126 359	59 252	11 380	2084	263	1114	8579	2494	481	12 669	45	346	101	19	512	910	67
Hubei	38 967	85 429	4828	15 521	90	117	4216	361	1221	5914	5	170	15	49	239	2102	156
Hunan	36 273	53 428	5231	10 477	61	75	1807	268	565	2714	3	73	11	23	110	227	17
Inner Mongolia	225 139	29 432	17 350	26 335	165	1246	2675	2387	3816	10 124	50	108	96	154	409	7077	525
Jiangsu	189 947	55 263	141	626	637	4062	19 409	75	350	23 896	164	784	3	14	965		
Jiangxi	26 976	25 154	1350	587	76	69	1051	85	39	1244	3	42	3	2	50		
Jilin	95 761	38 895	3948	2422	187	601	4007	616	398	5621	24	162	25	16	227	564	42
Liaoning	95 761	38 895	3948	2422	546	1755	11 707	1799	1162	16 424	71	473	73	47	663	296	22
Ningxia	53 381	11 525	662	592	209	375	1328	116	109	1927	15	54	5	4	78		
Qinghai	6166	4531	1076	780	170	35	425	153	117	729	1	17	6	5	29		
Shaanxi	60 902	33 625	4311	4933	194	396	3588	696	839	5519	16	145	28	34	223	3196	237
Shandong	199 887	115 266	4654	18 305	180	1208	11 436	699	2895	16 237	49	462	28	117	656	1036	77
Shanghai	37 199	8358	412	982	280	350	1290	96	242	1977	14	52	4	10	80		
Shanxi	125 466	43 747	12 454	8345	366	1540	8818	3800	2682	16 839	62	356	153	108	680	1092	81
Sichuan	27 899	60 105	3402	784	581	544	19 252	1650	401	21 846	22	777	67	16	882	460	34
Tianjin	37 627	9701	676	1705	280	354	1497	158	419	2428	14	60	6	17	98	823	61
Tibet	0	0	0	0		0	0	0	0	0	0	0	0	0	0		
Xinjiang	61 655	26 070	2550	2680	262	543	3770	558	618	5490	22	152	23	25	222		
Yunnan	31 698	28 526	3929	3834	199	211	3122	651	669	4654	9	126	26	27	188	1480	110
Zhejiang	108 519	30 508	530	628	637	2321	10 715	282	352	13 669	94	433	11	14	552	6768	502
Mainland China	2 198 991	1 092 498	121 730	151 953		20 640	159 950	24 884	27 409	232 875	835	6457	1002	1106	9406	38 764	2874
Hong Kong	10 126	2225	0	0	280	95	343	0	0	439	4	14	0	0	18		
Taiwan	46 731	9243	0	37	280	439	1426	0	9	1875	18	58	0	0	76		

Table 2. Emission factors of chlorine from coal combustion in China.

Economic sector	Boiler type	Pollution control technology	Energy allocation ratio (%)[a]	Chlorine release rate (%)	Removal efficiency from dust-removal facilities (%)	Removal efficiency from sulfate-removal facilities (%)
Power plant	Pulverized coal boiler	Cottrell	43	98.5[b]	5.1[b]	95.5[b]
	Pulverized coal boiler	Bag-type dust remover	43	98.5[b]	10.4[b]	95.5[b]
	Pulverized coal boiler	Wet-type dust remover	6	98.5[b]	60.0[c]	95.5[b]
	Grate furnace	Wet-type dust remover	7	99[e]	60.0[c]	95.5[b]
	Grate furnace	Mechanical dust collector	1	99[e]	25[f]	95.5[b]
Industry	Grate furnace	Wet-type dust remover	29	99[e]	60.0[c]	0
	Grate furnace	Mechanical dust collector	58	99[e]	25[f]	0
	Grate furnace	No	4	99[e]	0	0
	Fluidized bed boiler	Wet-type dust remover	9	99.6[d]	60.0[c]	0
Residential	Traditional stove	No	19	94[g]	0	0
	Reinforced stove	No	41	94[g]	0	0
	Tea bath	No	4	94[g]	0	0
Other	Grate furnace	No	100	99[e]	0	0

[a] From Jiang et al. (2005). [b] From Deng et al. (2014). [c] From Jiang et al. (2004). [d] From Lopez-Vilarino et al. (2003). [e] From Ruud Meij, personal communication, 1991. [f] From Mei et al. (2006). [g] From Iapalucci et al. (1969).

sulfate-removal facilities. The chlorine emission factors in power plant, industry, residential, and other categories were calculated based on the parameters given in Tables 1 and 2. They were then applied to estimate the HCl and Cl_2 emissions from coal combustion.

2.1.4 Development of the emission inventory

The HCl and Cl_2 emissions (Es) from coal combustion were estimated as follows:

$$E_{i,j} = M_{i,j} \times \mathrm{EF}_{i,j} \times \rho \times \frac{1}{\mathrm{MM}}, \tag{9}$$

where M represents coal consumption, MM denotes the ratios of the molar mass of chlorine atom to the molecular weight of HCl and Cl_2 (35.5/36.5 for HCl and 1 for Cl_2), and ρ is the chlorine proportion of HCl and Cl_2 in emitted flue gas. The flue gas contains chlorine species in the form of particulate Cl^- and gaseous HCl and Cl_2, which were formed through chemical transformation during coal combustion. An average chlorine proportion of about 86.3 and 3.6 % was reported respectively for HCl and Cl_2 in the flue gas samples, which were collected from six pulverized coal boiler units in four coal-fired power plants in China (Deng et al., 2014). We adopted this ρ (86.3 and 3.6 % respectively for HCl and Cl_2) when calculating HCl and Cl_2 emissions. Similar procedures were followed to estimate chlorine emissions in Hong Kong and Taiwan. Table 1 lists the calculated HCl and Cl_2 emissions from coal combustion in each region (columns 7–11 for HCl and columns 12–16 for Cl_2).

We employed the same resolution ($0.25° \times 0.25°$) as the one used in the MEIC for the meshed grid to develop the ACEIC. The HCl and Cl_2 emissions from each economic sector were spatially allocated into the center of each grid cell. To allocate the chlorine emissions from power plants, a database of the location of each point source was needed. We constructed the database following the procedures below: the chlorine emissions in each grid cell were determined using the emissions of chlorine in the region, multiplied by a ratio of SO_2 emissions from power plants in MIX (an Asian anthropogenic emission inventory) in each grid cell to the total emissions of SO_2 in the region. MIX was developed for the year 2010 to support the Model Intercomparison Study for Asia Phase III (MICS-Asia III) and the Task Force on Hemispheric Transport of Air Pollution (TF HTAP) (Li et al., 2015). MEIC emission was included in MIX. MIX data had five categories: power plant, industry, residential, transport and agriculture. In ACEIC, the locations and relative amount of chlorine emissions from power plants were assumed to be the same as those of SO_2 emissions from the power plants in MIX, though this hypothesis might lead to a small uncertainty. In this way, the spatial distributions of emissions of HCl and Cl_2 from coal combustion of power plants were then determined. Chlorine emissions from other sectors were spatially allocated based on population in 2012. The chlorine emissions in each grid cell were obtained using the chlorine emissions in the region, multiplied by the ratio of population in each grid cell to the total population in the region. The spatial distributions of HCl and Cl_2 emissions from coal combustion of power plant, industry, residential, and others are shown in Figs. S1 and S2 in the Supplement. The chlorine emission of each sector in eastern China was higher than that in western China.

2.2 Emission from prescribed waste incineration

2.2.1 Prescribed waste incineration database

Table 1 also lists the waste incineration from garbage disposal incinerators in each province/city from the China Urban-Rural Construction Statistical Yearbook (CURCSY, National Bureau of Statistics, 2012), which was used to estimate chlorine emissions from prescribed waste incineration. Note that the emissions of chlorine were calculated only for the regions with garbage disposal incinerators (a total of 22 regions in this study). The information (location and daily capacity) on the garbage disposal incinerators was obtained from the Information Platform for Municipal Solid Waste Incineration (www.waste-cwin.org).

2.2.2 The HCl emission factor for prescribed waste incineration

Domestic waste contains chlorine in materials such as vegetable matter, paper, plastic, dry cell batteries, and salt (Lightowlers and Cape, 1988). The chlorine content of municipal waste is 0.5 wt % on average. An unabated emission factor of $2.2\,\mathrm{g\,HCl\,kg^{-1}}$ for municipal solid waste was reported by Emmel et al. (1989), lower than that for ordinary household waste ($3.5\,\mathrm{g\,HCl\,kg^{-1}}$, D. Holland, personal communication, 1991). We adopted the former value ($2.2\,\mathrm{g\,HCl\,kg^{-1}}$) when estimating the HCl emission from prescribed waste incineration. The Cl_2 emission from prescribed waste incineration was not included due to unavailable data from the literature.

The net emission factor (EF) for prescribed waste incineration was estimated according to the following Eq. (10):

$$\mathrm{EF} = \mathrm{EF}_{\mathrm{raw}} \times (1 - \eta_{\mathrm{d}}) \times (1 - \eta_{\mathrm{s}}), \tag{10}$$

where $\mathrm{EF}_{\mathrm{raw}}$ is the unabated emission factor ($2.2\,\mathrm{g\,kg^{-1}}$) and η_{d} and η_{s} are the chlorine removal efficiency of dust-removal facilities and sulfate-removal facilities, respectively. We assumed that the control technology of garbage disposal incinerator was similar to the coal combustion of a power plant, and we hence used the average values of η_{s} and η_{d} data for the power plant sector in Table 2 to yield the HCl emission factor.

2.2.3 Development of the emission inventory

The HCl emission (E) for prescribed waste incineration were estimated as follows:

$$E_i = M_i \times \mathrm{EF}, \tag{11}$$

where i represents the province (municipality, autonomous region) and M denotes the amount of prescribed waste incineration. The estimated HCl emissions from prescribed waste incineration in each region are listed in Table 1.
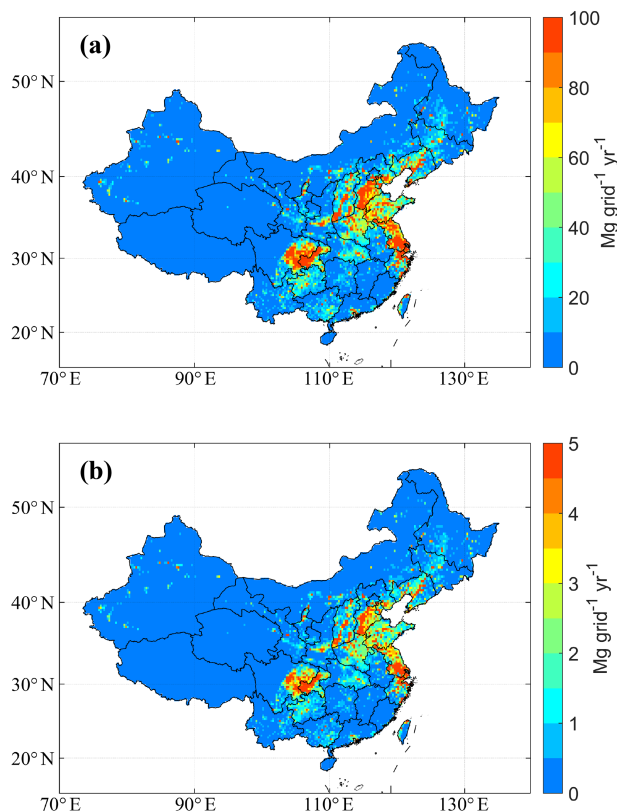

Figure 1. Spatial distribution of the emissions of hydrogen chloride **(a)** and molecular chlorine **(b)** in the ACEIC.

The HCl emission at each garbage disposal incinerator was obtained using the emission in the region, multiplied by the ratio of the daily capacity of each waste incineration plant to the total daily capacity of all plants in the region (Table 1). The HCl emissions at all the garbage disposal incinerators were then merged into a $0.25° \times 0.25°$ grid cell. The results show that high emissions from prescribed waste burning could be seen around the coastal region of eastern China (Fig. S3).

2.3 The anthropogenic chlorine emission inventory for China

2.3.1 The HCl and Cl$_2$ emissions

The ACEIC developed in this study included HCl and Cl_2 emissions from coal combustion and HCl emissions from prescribed waste incineration. Table 1 shows the chlorine emissions of all the regions in China, along with Hong Kong and Taiwan. The HCl and Cl_2 emissions from coal combustion in China in 2012 were estimated to be 232.9 and 9.4 Gg, respectively, and HCl emissions from prescribed waste burning were estimated to be 2.9 Gg. Figure 1a and b show the spatial distribution of the total HCl and Cl_2 emissions, respectively, where similar patterns were found, although in
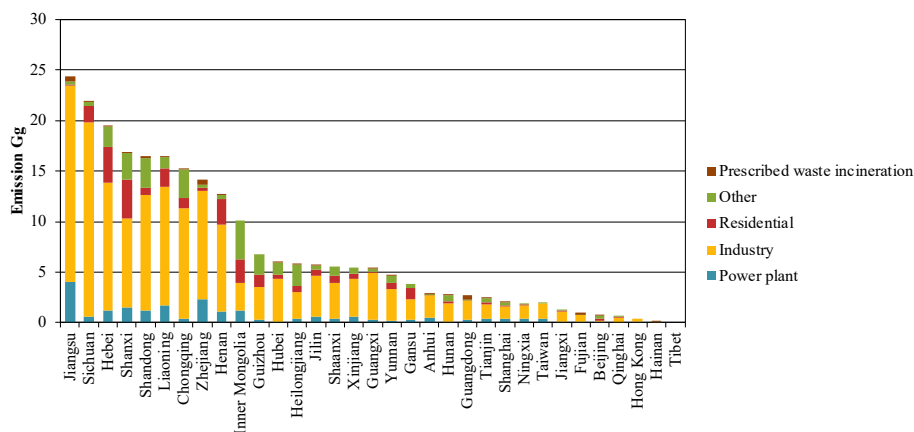
Figure 2. The HCl emission in the study region in 2012 from four economic sectors of coal combustion and from prescribed waste incineration.

general the HCl emission is almost 20 times higher than that of the Cl_2 emission. The North China Plain, the Yangtze River Delta (YRD), and the Sichuan Basin contributed spatially high chlorine emissions. The highest HCl emission was found in Jiangsu, followed by Sichuan and Hebei provinces (Fig. 2). Chlorine emissions were relatively low in South China, including Guangdong, Hunan, Fujian, Jiangxi, and Hainan, probably due to the low chlorine contents in coal used in those regions. The HCl emission from industry contributed to as high as 68 % of the total emissions, followed by others (12 %), residential (10 %), power plant (9 %), and prescribed waste incineration (1 %). Many industrial processes (e.g., iron and steel processing, nonferrous metals processing, cement production) that need coal burning are included in the industrial sector, leading to the highest source of HCl.

2.3.2 Comparison with other chlorine emission

The RCEI developed by McCulloch et al. (1999) was the only emission inventory for chlorine that included China, containing the chlorine emitted globally from coal combustion and waste incineration in 1990. The ACEIC developed in this study made progress in four ways based on the RCEI. (1) The ACEIC provides a more comprehensive database of coal combustion and prescribed waste incineration in China. The data in each province/city in China were taken from the CESY and the CURCSY in this study, which were more detailed than those in the RCEI that were from IEA energy statistics and only included the total amount of coal consumption in China. (2) The ACEIC has a higher resolution ($0.25° \times 0.25°$) than the RCEI ($1° \times 1°$), providing a higher spatial resolution for regional air quality modeling. (3) There are more emission factors. When estimating emission factors, the ACEIC included the removal rates of chlorine from dust-removal facilities and sulfate-removal facilities in China, while the RCEI did not, leading to higher estimated HCl emission in the RCEI. We estimated about 232.9 Gg HCl

emission in China in 2012 in ACEIC, only about one-quarter of that estimated from the RCEI (866.7 Gg). (4) The ACEIC accounts for Cl_2 emission. The ACEIC includes Cl_2 emission, which is also emitted during coal combustion in China based on the measurement by Deng et al. (2014).

In the following section, the ACEIC was incorporated into the CMAQ model to simulate the air quality in central and eastern China. It was evaluated by comparing the simulated and observed concentrations of chlorine species. In addition, the effect of chlorine emissions on tropospheric ozone formation was quantified to assess its importance in atmospheric chemistry in China. The refined and updated anthropogenic chlorine emission will help to evaluate the impact of chlorine emission on ozone formation in China.

3 Impact of chlorine emissions on tropospheric ozone formation

3.1 Model setting

The CMAQ model was developed by the United States Environmental Protection Agency (US EPA) to approach air quality as a whole by including state-of-the-science capabilities for modeling multiple air quality issues, including tropospheric ozone, fine particles, toxics, acid deposition, and visibility degradation (Byun and Schere, 2006). The latest version (5.1) was used in this study. Meteorological inputs were driven by the Weather Research and Forecasting (WRF) model. The meteorological boundary conditions and initial conditions of the WRF were provided by NCEP/NCAR final (FNL) reanalysis data ($1° \times 1°$). The modeling domain with 27 km horizontal resolution is shown in Fig. 3. The number of modeled layers was 40 and the highest layer can reach the top of 50 hPa. The CMAQ modeling domain covered central and eastern China, which was smaller than the WRF modeling domain, to reduce the effect of meteorological bound-
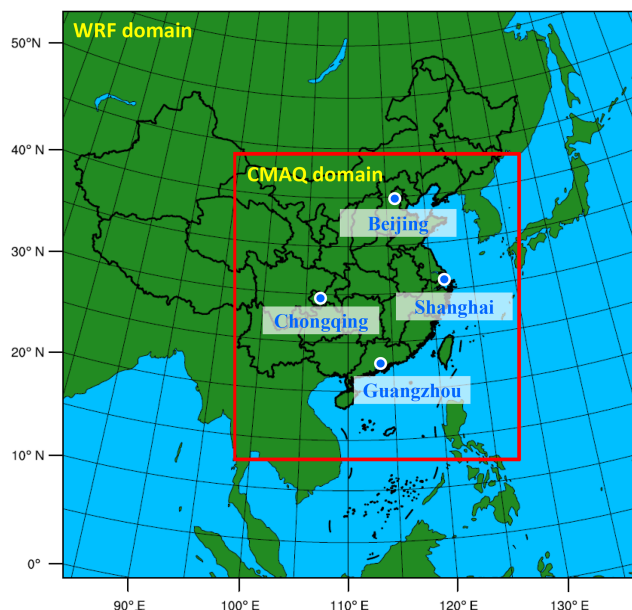
Figure 3. Modeling domain of WRF/CMAQ and the locations of typical sites: Beijing, Shanghai, Guangzhou, and Chongqing.

aries from the WRF model. The meteorology–chemistry interface processor (MCIP) was used to convert WRF outputs to CMAQ input format. The boundary conditions of chemical species for CMAQ were provided by the Model for Ozone and Related Chemical Tracers, version 4 (MOZART-4) results (http://www.acom.ucar.edu/wrf-chem/mozart.shtml).

In this study, anthropogenic and biogenic emissions were both included in the simulation. The MIX emission inventory (Li et al., 2017) was used in the simulation. International shipping emission was taken from the Hemispheric Transport Atmospheric Pollution (HTAP) emissions version 2.0 dataset (Janssens-Maenhout et al., 2015). Biogenic emission was calculated from the Model of Emissions of Gas and Aerosols from Nature (MEGAN) (Guenther et al., 2006). Additionally, sea salt emission was calculated during the simulation in the CMAQ model. The methods for estimating sea salt emission and its impact on aerosol chemical formation can be found in Liu et al. (2015). The SAPRC07TIC mechanism (Carter, 2010; Hutzell et al., 2012; Xie et al., 2013; Lin et al., 2013; Pye et al., 2015) was selected as the gas-phase chemical mechanism in the CMAQ model. ISORROPIA (Fountoukis and Nenes, 2007) was used to model the chemistry of inorganic aerosols. Detailed chlorine chemistry (including Eqs. 1–7) was considered in the CMAQ model.

The simulation was performed for November 2011. The spin-up time was 10 days (22–31 October) prior to November 2011. During the simulation period, China was controlled by high-pressure systems most of the time, which hindered the transport and diffusion of air pollutants.

Two experiments were set up to evaluate the impact of chlorine emission on tropospheric ozone formation. One ex-

periment included the ACEIC in the model (Base experiment), while the other experiment did not (NoCl experiment). The comparison of the Base and NoCl experiments could help to quantify the impacts of anthropogenic chlorine emissions. To include the ACEIC in the CMAQ model, the chlorine emissions from different economic sectors were temporally allocated in different ways. For the coal combustion from the power plant, industrial, and residential sectors, we distributed the total chlorine emissions between each month according to Wu (2009). In addition, the daily distributions of chlorine emissions from the power plant, industrial and residential sectors were allocated the same way as the allocations of the MIX inventory from the corresponding sectors. For the coal combustion from the other sectors, the total chlorine emission was divided equally into each month, each day, and each hour. Since the burning process of garbage disposal incinerators is similar to that of power plants, we assumed the same monthly and daily variation of prescribed waste incineration as that of the power plant sector. Four typical sites in four different regions were selected to analyze the diurnal variations of chlorine species: Beijing (BJ), Shanghai (SH), Guangzhou (GZ), and Chongqing (CQ). The locations of these sites are shown in Fig. 3.

3.2 Evaluation of chlorine species

3.2.1 HCl evaluation

Table 3 presents the comparison of modeled HCl concentrations to the observed values in China from available literature. It should be noted that the modeled and observed HCl concentrations were not paired in time and space. The modeled HCl concentrations in the Base and NoCl experiments in Beijing and Guangzhou were underestimated, while those in Shanghai and Hong Kong were overestimated. However, the modeled HCl concentrations from both experiments reasonably matched the observations in a similar magnitude. The difference between the modeled and observed HCl concentration in Beijing reduced when the ACEIC was incorporated into the model, implying the importance of anthropogenic emissions in this region.

3.2.2 Cl$_2$ evaluation

Reports on Cl$_2$ measurements in the atmosphere are sparse in the literature. The Cl$_2$ concentration was measured to be about 2.3 pptv on average in La Jolla (Finley and Saltzman, 2008) and 2.5–20 pptv with a 2-month mean of 3.5 pptv in Irvine, California. We estimated a monthly average concentration of 1–10 pptv (most of urban regions) in China in this study by incorporating the ACEIC into the CMAQ system for air quality modeling (Fig. 6a), which was reasonable compared to the observed values in North America. Cl$_2$ concentration was very low when anthropogenic chlorine emission was not included in the model (Fig. S8).

Table 3. A comparison of predicted HCl concentrations for the Base and NoCl experiments to observed data from literature*.

Location	Period	Observation	Base	NoCl	Reference
Beijing, China	Winter 2007	0.22	0.12	0.06	Ianniello et al. (2011)
Beijing, China	Summer 2007	0.45			Ianniello et al. (2011)
Beijing, China	Jul and Aug 2002 and 2003	0.6			Wu et al. (2009)
Beijing, China	Jul–Aug 2001	0.3–0.8			Yao et al. (2003)
Shanghai, China	Oct–Nov 2012	0.5	0.87	0.64	Shi et al. (2014)
Guangzhou, China	Oct–Nov 2004	2.8	1.10	1.05	Hu et al. (2008)
Hong Kong	Autumn 2000	0.8	1.27	1.18	Yao et al. (2006)

* Units are $\mu g\, m^{-3}$. Note that the observed and model values are not paired in time and space. Model predictions are taken from the general geographic areas of the observed data.

3.2.3 ClNO$_2$ evaluation

The highest ClNO$_2$ concentrations in China were observed throughout the Northern Hemisphere in the CMAQ simulation (Sarwar et al., 2014). Up to about 2000 pptv ClNO$_2$ concentration was measured in Hong Kong during the summer of 2012 (Tham et al., 2014) and in Tianjin during the summer of 2014 (Tham et al., 2016). We estimated a monthly average concentration of up to 1178 pptv ClNO$_2$ in China (Fig. 4g), which was comparable to the observed values.

3.3 Impact of chlorine emission on atmospheric oxidation

3.3.1 Impact of HCl emission

Figure 4a shows the spatial distribution of monthly average HCl concentration in the Base experiment. The HCl concentration over the ocean was higher than that over the land, due probably to the largest proportion of HCl emission from the dechlorination of sea salt aerosols (Graedel and Keene, 1995; Keene et al., 1999). The highest concentration of HCl was found in the South China Sea where sea salt emission was also high due to high wind speed and the downwind location (Fig. S4). The impact of chlorine emissions on HCl concentration is shown in Fig. 4b and c. The inclusion of the ACEIC in the model increased the HCl concentration by up to $1.7\,\mu g\, m^{-3}$ in inland China. The chlorine emissions accounted for up to 85.6 % of the HCl concentration in the Sichuan Basin (Fig. 4c). The dechlorination of sea salt aerosols transported to inland area was also considered an important proportion of HCl concentration, especially in South China and the coastal regions in East China (Fig. S5), where the impact of anthropogenic chlorine emission was low.

The spatial distribution of monthly mean concentrations of fine particulate Cl$^-$ is shown in Fig. 4d. A higher concentration was found in the North China Plain and the South China Sea. The concentrations of fine particulate Cl$^-$ increased by up to $2.0\,\mu g\, m^{-3}$ when anthropogenic chlorine emissions were included in the model (Fig. 4e). The increase

of fine particulate Cl$^-$ concentration was attributed to the gas–particle partitioning process of HCl and was sensitive to chlorine emissions, especially in the Sichuan Basin, contributing up to an 89 % increase (Fig. 4f).

The HCl concentrations were found to significantly increase in regions such as the Sichuan Basin and the YRD, consistent with the high anthropogenic chlorine emissions shown in Fig. 1a. However, the increase of HCl concentration was negligible in the North China Plain even though there was also high HCl emission, while surprisingly the concentration of particulate Cl$^-$ increased more significantly than that in the Sichuan Basin and the YRD. Volatile acidic species (i.e., HCl) can be partitioned into particles by neutralization reactions (Seinfeld and Pandis, 1998). Chlorine partitioning between gas and particle phases ([Cl$^-$]/([Cl$^-$] + [HCl])) was calculated and shown in Fig. 5. Higher chlorine partitioning meant that more HCl was transferred into particulate Cl$^-$. The spatial distribution of chlorine partitioning in the Base and NoCl experiment was almost the same, suggesting that the chlorine emissions had little impact on the rate of gas–particle conversion. Higher chlorine partitioning rates were found in the North China Plain than in other regions in inland China, where NH$_3$ emission was high (Fig. S6), leading to a significant increase of particulate Cl$^-$ concentration when the ACEIC was included in the model. Meanwhile, semi-volatile NH$_4$Cl is formed via a reversible phase equilibrium with NH$_3$ and HCl (Pio and Harrison, 1987). When the HCl emission was included in the model, HCl reacts with NH$_3$ to produce particulate NH$_4^+$ and Cl$^-$, provided that the NH$_3$ emission was sufficiently high. High NH$_3$ emission in the North China Plain accelerated the gas–particle transformation from NH$_3$ to particulate NH$_4^+$, leading to a decrease of NH$_3$ concentration and an increase of NH$_4^+$ concentration in PM$_{2.5}$ (up to -1.1 and $1.0\,\mu g\, m^{-3}$, respectively) (Fig. S7).

The spatial distribution of daily maximum 1 h ClNO$_2$ concentration is shown in Fig. 4g. The ClNO$_2$ concentration in the North China Plain, the Sichuan Basin, and the coastline along South China were significantly higher than those in other regions. The reservoir species ClNO$_2$ was formed through the heterogeneous reaction between Cl$^-$ and N$_2$O$_5$ on the aerosol surfaces. High Cl$^-$ concentrations would
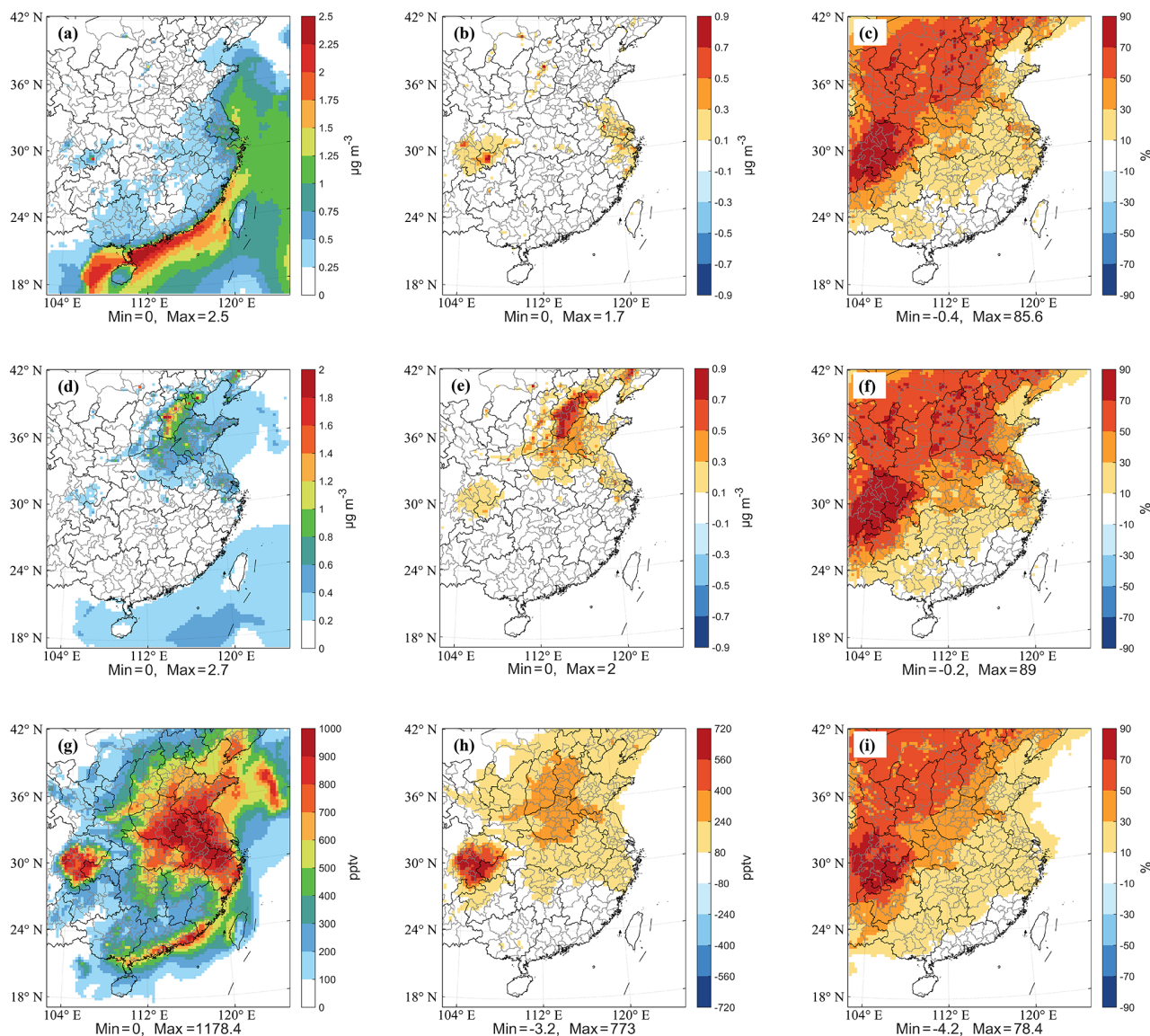
Figure 4. Spatial distributions of modeled HCl (**a**), fine particulate Cl^- (**d**), and daily maximum 1 h $ClNO_2$ (**g**) average concentrations in November 2011 in the Base experiment; the differences (Base minus NoCl) of modeled HCl (**b**), fine particulate Cl^- (**e**), and daily maximum 1h $ClNO_2$ (**h**) average concentrations in November 2011; the percent changes of the NoCl experiment to the Base experiment of modeled HCl (**c**), fine particulate Cl^- (**f**), and daily maximum 1 h $ClNO_2$ (**i**) average concentrations in November 2011.

accelerate the heterogeneous reaction rates, leading to enhanced $ClNO_2$ production. The inclusion of the ACEIC in the model increased the monthly daily maximum 1 h $ClNO_2$ concentration by up to 773 pptv in the whole domain, especially in the North China Plain and Sichuan Basin (Fig. 4h), highlighting the importance of anthropogenic chlorine emissions in $ClNO_2$ formation (up to 78.4 % of $ClNO_2$ production was related to anthropogenic chlorine emissions) (Fig. 4i).

3.3.2 Impact of Cl_2 emission

The spatial distribution of the monthly mean Cl_2 concentration is presented in Fig. 6a. As expected, high concentrations were found in regions with high Cl_2 emissions, including the Sichuan Basin, the YRD, and the North China Plain (Fig. 1b). The Cl_2 concentration was very low ($< 3.4 \times 10^{-3}$ pptv) when anthropogenic chlorine emissions were not included in the model (Fig. S8). The differences between Base and NoCl experiments (Fig. 6b) showed that Cl_2 was almost all from direct emissions; nearly 100 % of Cl_2 was originated from inland anthropogenic chlorine emissions (Fig. 6c). The
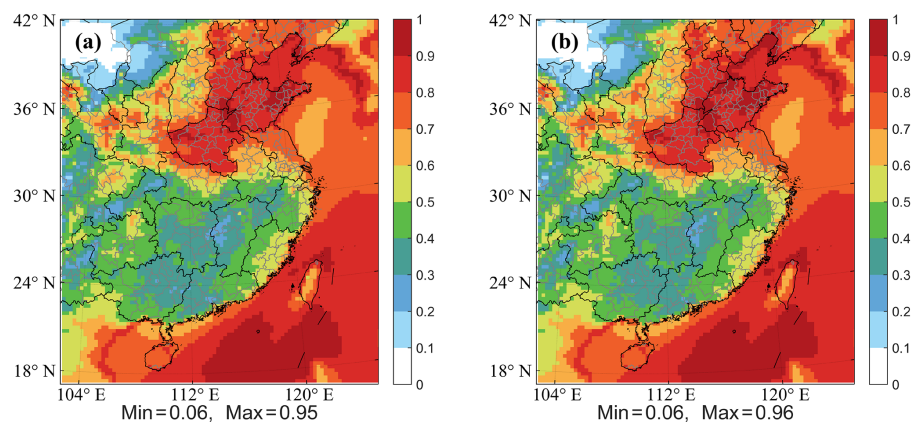
Figure 5. Spatial distribution of the monthly mean of chlorine partitioning ($[Cl^-]/([Cl^-]+[HCl])$) in the Base **(a)** and NoCl **(b)** experiment.
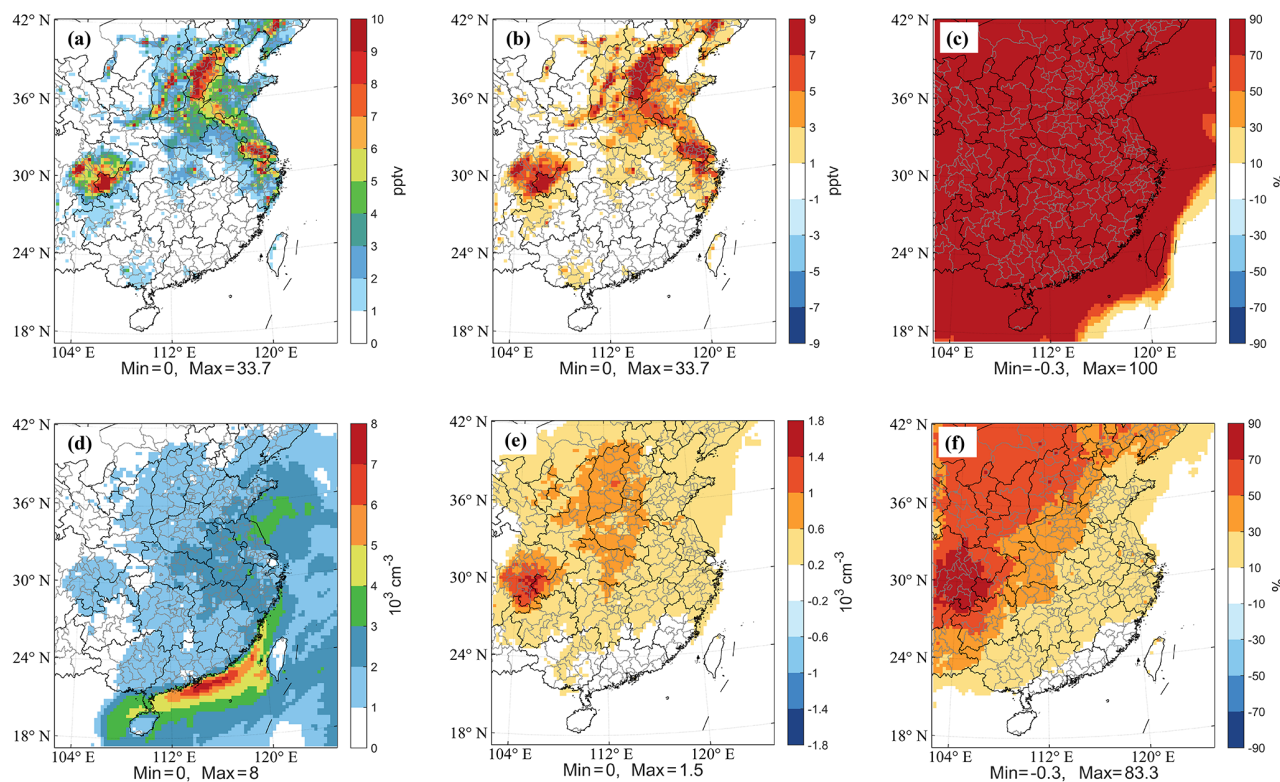
Figure 6. Spatial distributions of modeled Cl_2 **(a)** and Cl radical **(d)** average concentrations in November 2011 in the Base experiment; the differences (Base minus NoCl) of modeled Cl_2 **(b)** and Cl radical **(e)** average concentrations in November 2011; the percent changes of the NoCl experiment to the Base experiment of modeled Cl_2 **(c)** and Cl radical **(f)** average concentrations in November 2011.

results suggested that anthropogenic chlorine emission was a significant source of Cl_2, which should be included in air quality modeling in order to accurately model regional air quality.

3.3.3 Impact on Cl radicals

Both $ClNO_2$ (mainly from the heterogeneous reaction between particulate Cl^- and N_2O_5) and Cl_2 (mainly from di-

rect emissions) can photolyze to produce Cl radicals after sunrise (Eqs. 1 and 2). The diurnal variation of $ClNO_2$, Cl_2, and Cl radicals is presented in Fig. 7. The $ClNO_2$ concentration continued to drop and reached a minimal value between 12:00 and 16:00 but gradually increased after sunset due to the ceasing of photolysis and continuous accumulation of $ClNO_2$ from the heterogeneous reaction, and then it reached a peak just before sunrise. The Cl_2 concentration reached a
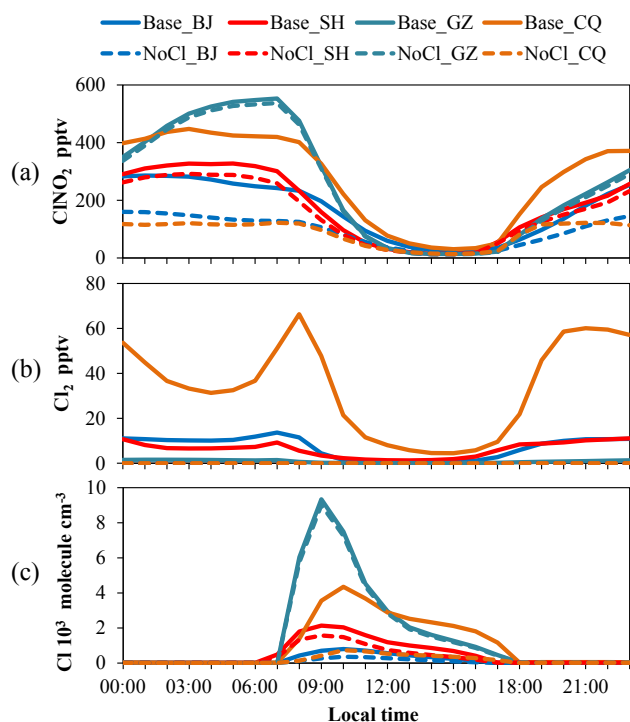
Figure 7. Diurnal variations of monthly mean concentrations of $ClNO_2$ **(a)**, Cl_2 **(b)**, and Cl radicals **(c)** in Beijing, Shanghai, Guangzhou, and Chongqing in the Base and NoCl experiments.

peak at about 08:00 and subsequently dropped substantially in the whole morning and early afternoon until 16:00 due to apparently photolysis. The Cl_2 concentration increased gradually after 16:00 and continued to accumulate during nighttime. The Cl radical concentration peaked in the morning due to the photolysis of Cl_2 and $ClNO_2$, while it was mainly formed through the reaction of HCl with OH in the afternoon when Cl_2 and $ClNO_2$ concentrations were very low. Similar diurnal cycles can be found at all sites; however, the impact of anthropogenic chlorine emissions at each site varied. Guangzhou and Shanghai sites could represent the coastal region, where the predominant sources of chlorine were from sea salt emission, while the Chongqing site could represent the inland region, where the predominant sources of chlorine were from coal combustion and waste incineration. The impact of anthropogenic chlorine emissions in Chongqing was higher than those in other regions.

The spatial distribution of Cl radical concentration is shown in Fig. 6d. A higher Cl radical concentration was found in the South China Sea, where high HCl concentration was found (Fig. S4a). The concentration of Cl radicals over the land reached up to 8×10^3 molecule cm^{-3}. The Cl concentrations increased by up to 1.5×10^3 molecule cm^{-3} in the whole domain when anthropogenic chlorine emissions were considered in the model (Fig. 6e). The chlorine emission contributed up to 83.3 % of Cl concentration (Fig. 6f).

3.4 Impact of chlorine emissions on tropospheric ozone formation

Atmospheric oxidation of VOCs initiated by the Cl radicals plays an important role in tropospheric ozone formation. The oxidation reaction was accelerated as the Cl concentration increased, leading to an increase of ozone and OH radical concentration. The OH radicals can in turn oxidize NO_x to produce particulate NO_3^-, resulting in the decrease of NO_x concentration. The monthly mean daily maximum 8 h O_3 concentration was high in South China, the Sichuan Basin, and southwestern China during November 2011 and increased by up to 2.0 ppbv (4.1 %) when anthropogenic chlorine emission was included (Fig. 8a–c), especially in central China. It is also shown that the impact of chlorine emission on 1 h O_3 concentration (Fig. S9) was similar to that of 8 h O_3. The impact of ACEIC was reasonable compared to the result reported in the Houston area (up to 3 ppbv increase of 1 h O_3 concentration) by Sarwar and Bhave (2007). The NO_x concentration was observed to be high in the North China Plain (Fig. 8d). It slightly decreased by up to 0.5 ppbv (6.1 %) when the anthropogenic chlorine emissions were included in the model (Fig. 8e–f). In particular, regions such as the North China Plain and the Sichuan Basin were significantly affected by the chlorine emissions. The NO_x concentration decreased, corresponding to the increase of O_3 concentration (Fig. 8b and e). This is attributed to the fact that more ozone production leads to the release of OH radicals when chlorine emissions were included in the model, which results in more oxidation of NO_x. The maximum impact of chlorine emissions on 1 h O_3 concentration is shown in Fig. 9. The largest increase of 1 h O_3 concentration was found along the Yangtze River, where the chlorine emission potentially increased the 1 h O_3 concentration by up to 7.7 ppbv.

4 Conclusions

The ACEIC was developed for the first time, which included HCl and Cl_2 from coal combustion and prescribed waste incineration. The HCl and Cl_2 emissions from coal combustion in China in 2012 were estimated to be 232.9 and 9.4 Gg, respectively, while HCl emission from prescribed waste incineration in China was estimated to be 2.9 Gg. The highest emissions of HCl and Cl_2 were found in the North China Plain, the Yangtze River Delta, and the Sichuan Basin. In the ACEIC, HCl emissions from coal combustion of industry contributed 68 % of the total emission, followed by others, residential, power plants, and prescribed waste incineration.

The modeling results with the ACEIC showed that the simulated HCl, Cl_2, and $ClNO_2$ agreed reasonably with the observed values. The inclusion of anthropogenic chlorine emissions in the model increased the concentration of fine particulate Cl^-, leading to an enhanced heterogeneous reaction of Cl^- with N_2O_5, which produced $ClNO_2$. Reaction of HCl
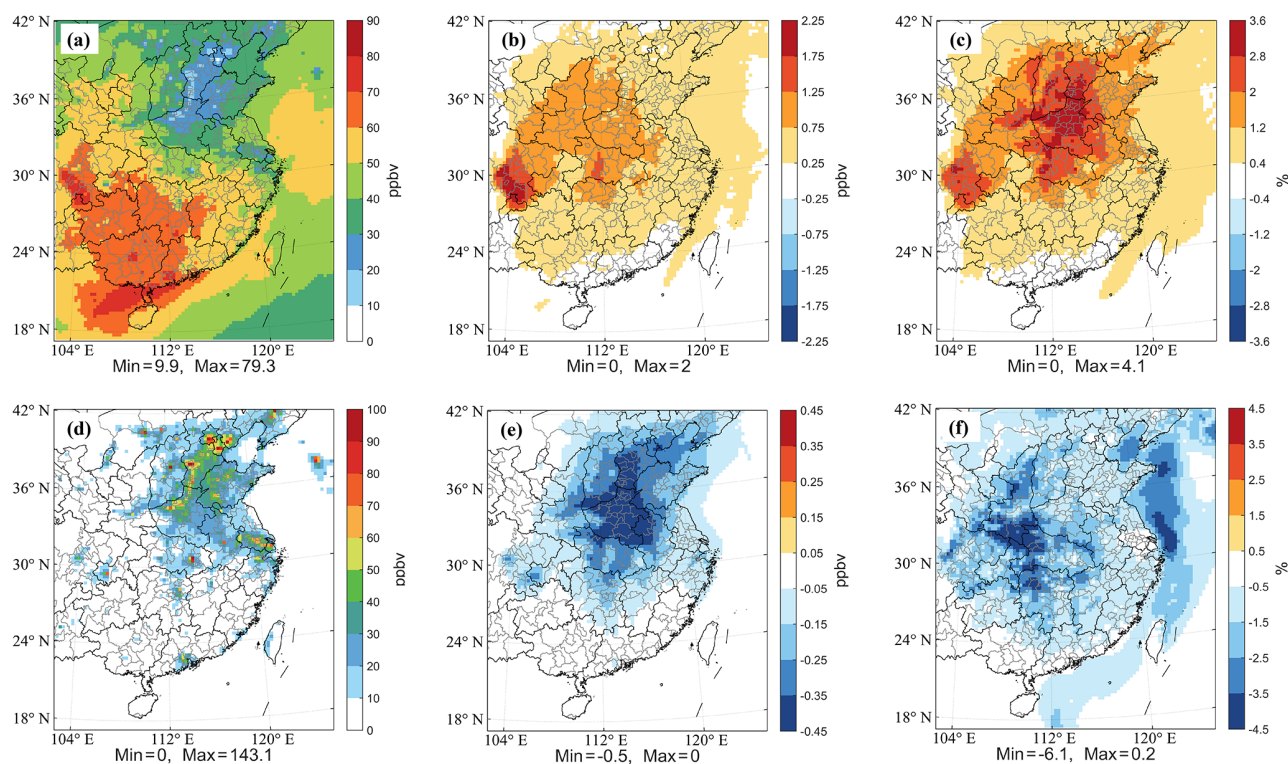
Figure 8. Spatial distributions of modeled daily maximum 8 h O_3 (a) and NO_x (d) average concentrations in November 2011 in the Base experiment; the differences (Base minus NoCl) of modeled daily maximum 8 h O_3 (b) and NO_x (e) average concentrations in November 2011; the percent changes of the Base experiment to the NoCl experiment of modeled daily maximum 8 h O_3 (c) and NO_x (f) average concentrations in November 2011.
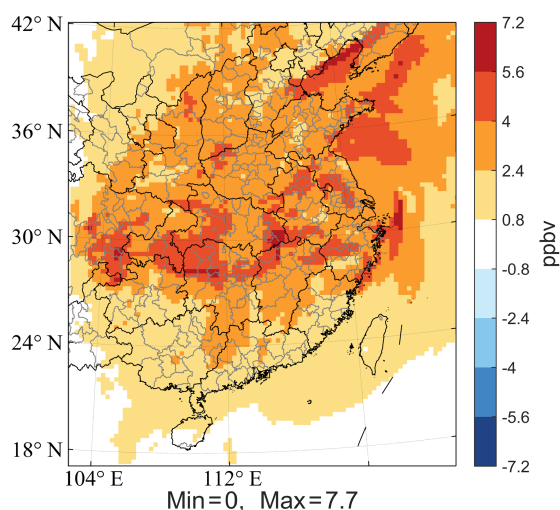

Figure 9. Spatial distribution of the maximum impact of chlorine emissions on 1 h O_3 concentration in November 2011.

with OH and photolysis of $ClNO_2$ and Cl_2 produce chlorine radicals. The monthly mean concentrations of fine particulate Cl^-, daily maximum 1 h $ClNO_2$, and Cl radicals increased by up to 2.0 µg m^{-3}, 773 pptv, and 1.5×10^3 molecule cm^{-3}

when anthropogenic chlorine emission was included in the model. In inland China, up to 89, 78.4, and 83.3 % of monthly mean concentrations of fine particulate Cl^-, daily maximum 1 h $ClNO_2$, and Cl radicals came from anthropogenic chlorine emissions, respectively.

The Cl radicals reacted with VOCs and potentially enhanced O_3 concentration. The monthly mean concentration of daily maximum 8 h O_3 increased by up to 2.0 ppbv (4.1 %) when the ACEIC was included in the model. The chlorine emission potentially increased the 1 h O_3 concentration by up to 7.7 ppbv in China. As the precursor of O_3, the monthly mean concentration of NO_x decreased by up to 0.5 ppbv (6.1 %). A significant increase of daily maximum 1 h O_3 was found in central China, corresponding to the region with a significant decrease of NO_x.

More attention should be paid to the influence of chlorine emissions. The impact of chlorine emissions on ozone formation might vary from season to season. In the future, other typical months will be simulated and analyzed. In addition, emissions of hydrogen chloride and molecular chlorine not only contribute to the increase of tropospheric ozone concentration, but they also enhance the concentrations of particulate NH_4^+. Further studies should focus on the impact of

chlorine emissions on secondary aerosol formation and deposition.

The Supplement related to this article is available online at https://doi.org/10.5194/acp-18-2709-2018-supplement.

References

Andreae, M. O., Atlas, E., Harris, G. W., Helas, G., de Koc, A., Koppmann, R., Maenhaut, W., Manø, S., Pollock, W. H., Rudolph, J., Scharffe, D., Schebeske, G., and Welling, M.: Methyl halide emissions from savanna fires in southern Africa, J. Geophys. Res., 101, 23603–23613, https://doi.org/10.1029/95JD01733, 1996

Aschmann, S. M. and Atkinson, R.: Rate constants for the gas-phase reactions of alkanes with Cl atoms at 296 ± 2 K, Int. J. Chem. Kinet., 27, 613–622, https://doi.org/10.1002/kin.550270611, 1995.

Bertram, T. H. and Thornton, J. A.: Toward a general parameterization of N_2O_5 reactivity on aqueous particles: the competing effects of particle liquid water, nitrate and chloride, Atmos. Chem. Phys., 9, 8351–8363, https://doi.org/10.5194/acp-9-8351-2009, 2009.

Byun, D. W. and Schere, K. L.: Review of the Governing Equations, Computational Algorithms, and Other Components of the Models-3 Community Multiscale Air Quality (CMAQ) Modeling System, Appl. Mech. Rev., 59, 51–77, https://doi.org/10.1115/1.2128636, 2006.

Carter, W. P. L.: Development of the SAPRC-07 chemical mechanism, Atmos. Environ., 44, 5324–5335, https://doi.org/10.1016/j.atmosenv.2010.01.026, 2010.

Chang, S. H. and Allen, D. T.: Atmospheric chlorine chemistry in southeast Texas: Impacts on ozone formation and control, Environ. Sci. Technol., 40, 251–262, https://doi.org/10.1021/es050787z, 2006.

Chang, S. H., McDonald-Buller, E., Kimura, Y., Yarwood, G., Neece, J., Russell, M., Tanaka, P., and Allen, D.: Sensitivity of urban ozone formation to chlorine emission estimates, Atmos. Environ., 36, 4991–5003, https://doi.org/10.1016/S1352-2310(02)00573-3, 2002.

Chen, L. H.: Study on environmental geochemistry of chlorine in Chinese coals, M.S. thesis, Nanchang University, China, 46 pp., 2010.

Deng, S., Zhang, C., Liu, Y., Cao, Q., Xu, Y. Y., Wang, H. L., and Zhang, F.: A full-scale field study on chlorine emission of pulverized coal-fired power plants in China, Res. Environ. Sci., 27, 127–133, https://doi.org/10.13198/j.issn.1001-6929.2014.02.03, 2014 (in Chinese).

Emmel, T. E., Waddell, J. T., and Adams, R. C.: Acidic emissions control technology and costs, Pollution Technology Review, 168. NC, USA, Radian Corporation, 155 pp., 1989.

Faxon, C. B. and Allen, D. T.: Chlorine chemistry in urban atmospheres: a review, Environ. Chem., 10, 221–233, https://doi.org/10.1071/EN13026, 2013.

Finley, B. D. and Saltzman, E. S.: Observations of Cl_2, Br_2, and I_2 in coastal marine air, J. Geophys. Res.-Atmos., 113, D21301, https://doi.org/10.1029/2008JD010269, 2008.

Fountoukis, C. and Nenes, A.: ISORROPIA II: a computationally efficient thermodynamic equilibrium model for K^+-Ca^{2+}-Mg^{2+}-NH_4^+-Na^+-SO_4^{2-}-NO_3^--Cl^--H_2O aerosols, Atmos. Chem. Phys., 7, 4639–4659, https://doi.org/10.5194/acp-7-4639-2007, 2007.

Graedel, T. E. and Keene, W. C.: Tropospheric budget of reactive chlorine, Global Biogeochem. Cy., 9, 47–77, https://doi.org/10.1029/94GB03103, 1995.

Guenther, A., Karl, T., Harley, P., Wiedinmyer, C., Palmer, P. I., and Geron, C.: Estimates of global terrestrial isoprene emissions using MEGAN (Model of Emissions of Gases and Aerosols from Nature), Atmos. Chem. Phys., 6, 3181–3210, https://doi.org/10.5194/acp-6-3181-2006, 2006.

Hu, M., Wu, Z. J., Slanina, J., Lin, P., Liu, S., and Zeng, L. M.: Acidic gases, ammonia and water-soluble ions in $PM_{2.5}$ at a coastal site in the Pearl River Delta, China, Atmos. Environ., 42, 6310–6320, https://doi.org/10.1016/j.atmosenv.2008.02.015, 2008.

Hutzell, W. T., Luecken, D. J., Appel, K. W., and Carter, W. P. L.: Interpreting predictions from the SAPRC07 mechanism based on regional and continental simulations, Atmos. Environ., 46, 417–429, https://doi.org/10.1016/j.atmosenv.2011.09.030, 2012.

Ianniello, A., Spataro, F., Esposito, G., Allegrini, I., Hu, M., and Zhu, T.: Chemical characteristics of inorganic ammonium salts in $PM_{2.5}$ in the atmosphere of Beijing (China), Atmos. Chem. Phys., 11, 10803–10822, https://doi.org/10.5194/acp-11-10803-2011, 2011.

Iapalucci, T. L., Demski, R. J., and Bienstock, D.: Chlorine in coal combustion, US Bureau of Mines, Report of Investigations, US-BMRI7260, Pittsburgh, USA, vp., 1969.

IEA (International Energy Agency): Energy Statistics of OECD countries and non-OECD countries, IEA, Paris, available at http://www.iea.org/statistics (last access: February 2018), 2012.

Impey, G. A., Shepson, P. B., Hastie, D. R., and Barrie, L. A.: Measurement technique for the determination of photolyzable chlorine and bromine in the atmosphere, J. Geophys. Res., 102, 15999–16004, https://doi.org/10.1029/97JD00850, 1997.

Janssens-Maenhout, G., Crippa, M., Guizzardi, D., Dentener, F., Muntean, M., Pouliot, G., Keating, T., Zhang, Q., Kurokawa, J., Wankmüller, R., Denier van der Gon, H., Kuenen, J. J. P., Klimont, Z., Frost, G., Darras, S., Koffi, B., and Li, M.: HTAP_v2.2: a mosaic of regional and global emission grid maps for 2008 and 2010 to study hemispheric transport of air pollution, Atmos. Chem. Phys., 15, 11411–11432, https://doi.org/10.5194/acp-15-11411-2015, 2015.

Jiang, J. K., Hao, J. M., Wu, Y., David, G. S., Duan, L., and Tian, H. Z.: Development of mercury emission inventory from coal combustion in China, Environ. Sci., 26, 34–39, https://doi.org/10.13227/j.hjkx.2005.02.007, 2005 (in Chinese).

Jiang, X. G., Li, X. P., Li, Q., Chi, C., and Yan, J. H.: Industrial experiment study on chloride emission and dechlorination technology, Thermal Power Generation, 2004, 37–39, 2004 (in Chinese).

Keene, W. C., Khalil, M. A. K., Erickson, D. J., McCulloch, A., Graedel, T. E., Lobert, J. M., Aucott, M. L., Gong, S. L., Harper, D. B., and Kleiman, G.: Composite global emissions of reactive chlorine from anthropogenic and natural sources: Reactive Chlorine Emission Inventory, J. Geophys. Res.-Atmos., 104, 8429–8440, https://doi.org/10.1029/1998JD100084, 1999.

Lawler, M. J., Sander, R., Carpenter, L. J., Lee, J. D., von Glasow, R., Sommariva, R., and Saltzman, E. S.: HOCl and Cl_2 observations in marine air, Atmos. Chem. Phys., 11, 7617–7628, https://doi.org/10.5194/acp-11-7617-2011, 2011.

Lightowlers, P. J. and Cape, J. N.: Sources and fate of atmospheric HCl in the UK and western Europe, Atmos. Environ., 22, 7–15, https://doi.org/10.1016/0004-6981(88)90294-6, 1988.

Li, M., Zhang, Q., Kurokawa, J.-I., Woo, J.-H., He, K., Lu, Z., Ohara, T., Song, Y., Streets, D. G., Carmichael, G. R., Cheng, Y., Hong, C., Huo, H., Jiang, X., Kang, S., Liu, F., Su, H., and Zheng, B.: MIX: a mosaic Asian anthropogenic emission inventory under the international collaboration framework of the MICS-Asia and HTAP, Atmos. Chem. Phys., 17, 935–963, https://doi.org/10.5194/acp-17-935-2017, 2017.

Li, Q., Zhang, L., Wang, T., Tham, Y. J., Ahmadov, R., Xue, L., Zhang, Q., and Zheng, J.: Impacts of heterogeneous uptake of dinitrogen pentoxide and chlorine activation on ozone and reactive nitrogen partitioning: improvement and application of the WRF-Chem model in southern China, Atmos. Chem. Phys., 16, 14875–14890, https://doi.org/10.5194/acp-16-14875-2016, 2016.

Lin, Y. H., Zhang, H., Pye, H. O. T., Zhang, Z., Marth, W. J., Park, S., Arashiro, M., Cui, T., Budisulistiorini, S. H., Sexton, K.G., Vizuete, W., Xie, Y., Luecken, D. J., Piletic, I. R., Edney, E. O., Bartolotti, L. J., Gold, A., and Surratt, J. D.: Epoxide as a precursor to secondary organic aerosol formation from isoprene photooxidation in the presence of nitrogen oxides, P. Natl. Acad. Sci. USA, 110, 6718–6723, https://doi.org/10.1073/pnas.1221150110, 2013.

Liu, Y. M., Zhang, S. T., Fan, Q., Wu, D., Chan, P. W., Fan, S. J., Feng, Y. R., and Hong, Y. Y.: Accessing the impact of sea-salt emissions on aerosol chemical formation and deposition over Pearl River Delta, China, Aerosol Air Qual. Res., 15, 2232–2245, https://doi.org/10.4209/aaqr.2015.02.0127, 2015.

Lobert, J. M., Keene, W. C., Logan, J. A., and Yevich, R.: Global chlorine emissions from biomass burning: Reactive Chlorine Emissions Inventory, J. Geophys. Res.-Atmos., 104, 8373–8389, https://doi.org/10.1029/1998JD100077, 1999.

Lopez-Vilarino, J. M., Fernandez-Martinez, G., Turnes-Carou, I., Muniategui-Lorenzo, S., Lopez-Mahia, P., and Prada-Rodriguez, D.: Behavior of fluorine and chlorine in Spanish coal fired power plants with pulverized coal boilers and fluidized bed boiler, Environ. Technol., 24, 687–692, https://doi.org/10.1080/09593330309385604, 2003.

Lu, B. H.: Occurrence characteristics of fluorine and chlorine in coal seam in China, Coal Geology and Exploration, 24, 9–12, 1996 (in Chinese).

McCulloch, A., Aucott, M. L., Benkovitz, C. M., Graedel, T. E., Kleiman, G., Midgley, P. M., and Li, Y. F.: Global emissions of hydrogen chloride and chloromethane from coal combustion, incineration and industrial activities: Reactive Chlorine Emissions Inventory, J. Geophys. Res.-Atmos., 104, 8391–8403, https://doi.org/10.1029/1999JD900025, 1999.

Mei, H. S., Chen, D. Z., Liu, Y., and Mao, Q. X.: Incineration flue gas purification in a laboratory scale cyclone scrubber, Journal of Tongji University (Natural Science), 34, 953–959, 2006 (in Chinese).

National Bureau of Statistics: China Urban-Rural Construction Statistical Yearbook 2012, China Statistics Press, Beijing, 2012.

National Bureau of Statistics: China Energy Statistical Yearbook 2013, China Statistics Press, Beijing, 2013.

Nelson, L., Rattigan, O., Neavyn, R., Sidebottom, W., Treacy, J., and Nielsen, O. J.: Absolute and relative rate constants for the reactions of hydroxyl radicals and chlorine atoms with a series of aliphatic alchohols and ethers at 298K, Int. J. Chem. Kinet., 22, 1111–1126, https://doi.org/10.1002/kin.550221102, 1990.

Pio, C. A. and Harrison, R. M.: Vapour pressure of ammonium chloride aerosol: effect of temperature and humidity, Atmos. Environ., 21, 2711–2715, https://doi.org/10.1016/0004-6981(87)90203-4, 1987.

Pye, H. O. T., Luecken, D. J., Xu, L., Boyd, C. M., Ng, N. L., Baker, K., Ayres, B. A., Bash, J. O., Baumann, K., Carter, W. P. L., Edgerton, E., Fry, J. L., Hutzell, W. T., Schwede, D., and Shepson, P. B.: Modeling the current and future roles of particulate organic nitrates in the southeastern United States, Environ. Sci. Technol., 49, 14195–14203, https://doi.org/10.1021/acs.est.5b03738, 2015.

Riedel, T. P., Bertram, T. H., Crisp, T. Q., Williams, E. J., Lerner, B. M., Vlasenko, A., Li, S. M., Gilman, J., de Gouw, J., Bon, D. M., Wagner, N. L., Brown, S. S., and Thornton, J. A.: Nitryl chloride and molecular chlorine in the coastal marine boundary layer, Environ. Sci. Technol., 46, 10463–10470, https://doi.org/10.1021/es204632r, 2012.

Robert, J. M., Osthoff, H. D., Brown, S. S., Ravishankara, A. R., Coffman, D., Quinn, P., and Bates, T.: Laboratory studies of products of N_2O_5 uptake on Cl^- containing substrates, Geophys. Res. Lett., 36, L20808, https://doi.org/10.1029/2009GL040448, 2009.

Sarwar, G. and Bhave, P. V.: Modeling the effect of chlorine emissions on ozone levels over the eastern United States, J. Appl. Meteorol. Clim., 46, 1009–1019, https://doi.org/10.1175/JAM2519.1, 2007.

Sarwar, G., Simon, H., Xing, J., and Mathur, R.: Importance of tropospheric ClNO$_2$ chemistry across the Northern Hemisphere, Geophys. Res. Lett., 41, 4050–4058, https://doi.org/10.1002/2014GL059962, 2014.

Seinfeld, J. H. and Pandis, S. N.: Atmospheric Chemistry and Physics, John Wiley & Sons, Inc., New York, 1998.

Shi, Y., Chen, J. M., Hu, D. W., Wang, L., Yang, X., and Wang, X. M.: Airborne submicron particulate (PM$_1$) pollution in Shanghai, China: Chemical variability, formation/dissociation of associated semi-volatile components and the impacts on visibility, Sci. Total Environ., 473, 199–206, https://doi.org/10.1016/j.scitotenv.2013.12.024, 2014.

Spicer, C. W., Plastridge, R. A., Foster, K. L., Finlayson-Pitts, B. J., Bottenheim, J. W., Grannas, A. M., and Shepson, P. B.: Molecular halogens before and during ozone depletion events in the Arctic at polar sunrise: concentrations and sources, Atmos. Environ., 36, 2721–2731, https://doi.org/10.1016/S1352-2310(02)00125-5, 2002.

Tang, X. Y. and Chen, P.: Chlorine in coal of China, Coal Geology of China, 14, 33–36, 2002 (in Chinese).

Tham, Y. J., Yan, C., Xue, L. K., Zha, Q. Z., Wang, X. F., and Wang, T.: Presence of high nitryl chloride in Asian coastal environment and its impact on atmospheric photochemistry, Chinese Sci. Bull., 59, 356–359, https://doi.org/10.1007/s11434-013-0063-y, 2014.

Tham, Y. J., Wang, Z., Li, Q., Yun, H., Wang, W., Wang, X., Xue, L., Lu, K., Ma, N., Bohn, B., Li, X., Kecorius, S., Größ, J., Shao, M., Wiedensohler, A., Zhang, Y., and Wang, T.: Significant concentrations of nitryl chloride sustained in the morning: investigations of the causes and impacts on ozone production in a polluted region of northern China, Atmos. Chem. Phys., 16, 14959–14977, https://doi.org/10.5194/acp-16-14959-2016, 2016.

Wang, L., Arey, J., and Atkinson, R.: Reactions of chlorine atoms with a series of aromatic hydrocarbons, Environ. Sci. Technol., 39, 5302–5310, https://doi.org/10.1021/es0479437, 2005.

Wiedinmyer, C., Yokelson, R. J., and Gullett, B. K.: Global emissions of trace gases, particulate matter, and hazardous air pollutants from open burning of domestic waste, Environ. Sci. Technol., 48, 9523–9530, https://doi.org/10.1021/es502250z, 2014.

Wingenter, O. W., Blake, D. R., Blake, N. J., Sive, B. C., Rowland, F. S., Atlas, E., and Flocke, F.: Tropospheric hydroxyl and atomic chlorine concentrations, and mixing timescales determined from hydrocarbon and halocarbon measurements made over the Southern Ocean, J. Geophys. Res.-Atmos., 104, 21819–21828, https://doi.org/10.1029/1999JD900203, 1999.

Wu, X. L.: The study of air pollution emission inventory in Yangtze Delta, M.S. thesis, Fudan University, China, 94 pp., 2009.

Wu, Z. J., Hu, M., Shao, K. S., and Slanina, J.: Acidic gases, NH$_3$ and secondary inorganic ions in PM$_{10}$ during summertime in Beijing, China and their relation to air mass history, Chemosphere, 76, 1028–1035, https://doi.org/10.1016/j.chemosphere.2009.04.066, 2009.

Xie, Y., Paulot, F., Carter, W. P. L., Nolte, C. G., Luecken, D. J., Hutzell, W. T., Wennberg, P. O., Cohen, R. C., and Pinder, R. W.: Understanding the impact of recent advances in isoprene photooxidation on simulations of regional air quality, Atmos. Chem. Phys., 13, 8439–8455, https://doi.org/10.5194/acp-13-8439-2013, 2013.

Yao, X. H., Lau, A. P. S., Fang, M., Chan, C. K., and Hu, M.: Size distributions and formation of ionic species in atmospheric particulate pollutants in Beijing, China: 1 – inorganic ions, Atmos. Environ., 37, 2991–3000, https://doi.org/10.1016/S1352-2310(03)00255-3, 2003.

Yao, X. H., Ling, T. Y., Fang, M., and Chan, C. K.: Comparison of thermodynamic predictions for in situ pH in PM$_{2.5}$, Atmos. Environ., 40, 2835–2844, https://doi.org/10.1016/j.atmosenv.2006.01.006, 2006.

Young, C. J., Washenfelder, R. A., Edwards, P. M., Parrish, D. D., Gilman, J. B., Kuster, W. C., Mielke, L. H., Osthoff, H. D., Tsai, C., Pikelnaya, O., Stutz, J., Veres, P. R., Roberts, J. M., Griffith, S., Dusanter, S., Stevens, P. S., Flynn, J., Grossberg, N., Lefer, B., Holloway, J. S., Peischl, J., Ryerson, T. B., Atlas, E. L., Blake, D. R., and Brown, S. S.: Chlorine as a primary radical: evaluation of methods to understand its role in initiation of oxidative cycles, Atmos. Chem. Phys., 14, 3427–3440, https://doi.org/10.5194/acp-14-3427-2014, 2014.

Zhao, F. H., Ren, D. Y., and Wang, Z.: Geochemical characteristics and step-by-step extraction of chlorine in coal, Journal of China University of Mining and Technology, 28, 61–64, 1999 (in Chinese).